

Domain-Adversarial and -Conditional State Space Model for Imitation Learning

Ryo Okumura¹, Masashi Okada¹ and Tadahiro Taniguchi^{1,2}

¹Panasonic Corporation

²Ritsumeikan University

{okumura.ryo001, okada.masashi001}@jp.panasonic.com, taniguchi@em.ci.ritsumeikan.ac.jp

Abstract

State representation learning (SRL) in partially observable Markov decision processes has been studied to learn abstract features of data useful for robot control tasks. For SRL, acquiring domain-agnostic states is essential for achieving efficient imitation learning (IL). Without these states, IL is hampered by domain-dependent information useless for control. However, existing methods fail to remove such disturbances from the states when the data from experts and agents show large domain shifts. To overcome this issue, we propose a domain-adversarial and -conditional state space model (DAC-SSM) that enables control systems to obtain domain-agnostic and task- and dynamics-aware states. DAC-SSM jointly optimizes the state inference, observation reconstruction, forward dynamics, and reward models. To remove domain-dependent information from the states, the model is trained with domain discriminators in an adversarial manner, and the reconstruction is conditioned on domain labels. We experimentally evaluated the model predictive control performance via IL for continuous control of sparse reward tasks in simulators and compared it with the performance of the existing SRL method. The agents from DAC-SSM achieved performance comparable to experts and more than twice the baselines. We conclude domain-agnostic states are essential for IL that has large domain shifts and can be obtained using DAC-SSM.

1 Introduction

State representation learning (SRL) [Lesort *et al.*, 2018] has been studied to obtain compact and expressive representation of robot control tasks from high-dimensional sensor data, such as images. Appropriate state representation enables agents to achieve high performance for discrete and continuous control tasks from games [Ha and Schmidhuber, 2018] to real robots [Wang *et al.*, 2019]. Sequential state space models have been shown to improve the performance and sample efficiency of robot control tasks in partially observable Markov

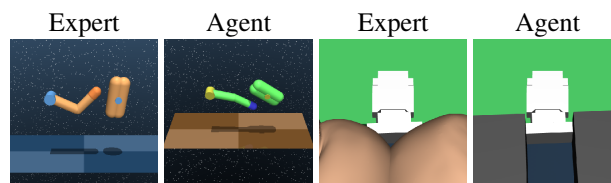


Figure 1: Examples of domain shifts between an expert and agent. We define the domain shifts as control-irrelevant changes in data like appearance. Colors, backgrounds and viewing angles are different between the two images on the left side. In the other images on the right side, unseen objects in one domain, human fingers in these examples, appear in the other domain.

decision processes (POMDPs). The deep planning network (PlaNet) [Hafner *et al.*, 2018] is a planning methodology in the latent space that is trained with a task- and dynamics-aware state space model called a recurrent state space model (RSSM). RSSM jointly optimizes the state inference, observation reconstruction, forward dynamics, and reward models. They have performed model predictive control (MPC) [Garcia *et al.*, 1989; Okada and Taniguchi, 2019] for planning in the obtained state space on RSSM.

Acquiring domain-agnostic states is essential for achieving efficient imitation learning (IL). Without the domain-agnostic states, IL is hampered by domain-dependent information, which is useless for control. In the context of IL, it is natural to assume that the data from experts and agents have domain shifts [Torabi *et al.*, 2019]. However, the current SRL methods [Hafner *et al.*, 2018; Lee *et al.*, 2019a] fail to remove such disturbances from the states when the domain shifts are large. In IL, a discriminator serves as an imitation reward function to distinguish the state-action pairs of the experts from those of the agents [Ho and Ermon, 2016]. If the obtained states are NOT domain-agnostic, the discriminator is disturbed by the domain-dependent information, which is eye-catching but unrelated to the control and tasks. As a result, the imitation reward becomes unsuitable for the control, and IL will be disrupted. Figure 1 shows examples of domain shifts between the data from an expert and agent. We define the domain shifts as control-irrelevant changes of the data like appearance: e.g. colors, textures, backgrounds, viewing angles, and objects that are unrelated to the control. The domain shifts are, for example, caused by changing camera settings,

location of data collection, appearance of the robot and so on. The domain shifts are also caused when unseen objects in one domain appear in the other domain. For example, an operator will be present in the expert images when she/he makes demonstrations via the direct teaching mode of a robot. In this case, the existence of the operator in the images is the cause of the domain shifts.

To overcome this problem, in this paper, we propose a domain-agnostic and task- and dynamics-aware SRL model, called a domain-adversarial and -conditional state space model (DAC-SSM). DAC-SSM builds on RSSM, and it is trained with a domain discriminator and expert discriminator. To remove the domain-dependent information from the states, (1) the state space is trained with the domain discriminator in an adversarial manner, and (2) the encoder and decoder of DAC-SSM are conditioned on domain labels. The domain discriminator is trained to identify which domain the acquired states belong to. The negative loss function of the domain discriminator, called the domain confusion loss [Tzeng *et al.*, 2014], is added to the loss function of the state space. To reduce the domain confusion loss, the states are trained to be domain-agnostic. In other words, due to the domain confusion loss, DAC-SSM is trained to inference the states that have few clues for the domain discriminator to distinguish domain of the states. Moreover, the states are disentangled by conditional domain labels for the encoder and decoder, like conditional variational autoencoders (CVAE) [Kingma *et al.*, 2014]. Owing to the disentanglement, the domain-dependent information is eliminated from the state representation. Because DAC-SSM jointly optimizes the state inference, observation reconstruction, forward dynamics, and reward models, the obtained states are also task- and dynamics-aware as well as domain-agnostic. To the best of our knowledge, there are no studies that have combined the domain adversarial training with SRL for control tasks.

The main contribution of this paper is implementation and experiments to demonstrate that the obtained state representation via DAC-SSM is suitable for IL with the large domain shifts. We compared DAC-SSM to the existing SRL methods in terms of MPC performance via IL for continuous control sparse reward tasks in the MuJoCo physics simulator [Todorov *et al.*, 2012]. The agents in DAC-SSM achieved a performance comparable to the expert and more than twice that of the baselines.

2 Related studies

State representation learning for POMDPs

The sequential state space model has been studied to solve the tasks in POMDPs. Lee *et al.* proposed a sequential latent variable model that propagates historical information from a control system via contextual stochastic states [Lee *et al.*, 2019a]. They jointly optimized the actor and critic using the state space model. Gangwani *et al.* jointly optimized the expert discriminator using policy, forward and inverse dynamics, and action models to obtain task- and dynamics-aware state representation [Gangwani *et al.*, 2019]. Their state representation, however, is not domain-agnostic.

Domain-agnostic feature representation

Domain-agnostic feature representation has been obtained by domain-adversarial training or by disentangling the latent space [Gonzalez-Garcia *et al.*, 2018]. The domain-adversarial training is a simple and effective approach to extract feature representation which is unrelated to the domains of data. Tzeng *et al.* added the domain confusion loss to the loss function of the feature extractor [Tzeng *et al.*, 2014]. Ganin *et al.* introduced a gradient reversal layer to back-propagate a negative gradient of the domain discriminator loss to the feature extractor [Ganin *et al.*, 2015]. CVAE is a well-known method that is able to disentangle domain-dependent information from the latent spaces. They made the encoder and decoder conditional on domain labels to obtain the domain-agnostic latent variables [Kingma *et al.*, 2014].

Imitation learning (IL)

IL [Schaal, 1999] is a powerful and accepted approach that makes the agents mimic expert behavior by using a set of demonstrations of tasks. Ho and Ermon proposed an IL framework called Generative Adversarial Imitation Learning (GAIL) [Ho and Ermon, 2016]. In GAIL, imitation rewards are computed by the expert discriminator, which distinguishes if a state-action pair is generated by an agent policy or from the expert demonstrations. They formulated a joint process of reinforcement learning and inverse reinforcement learning as a two-player game of the policy and discriminator, analogous to Generative Adversarial Networks [Goodfellow *et al.*, 2014]. GAIL has been shown to solve complex high-dimensional continuous control tasks [Kostrikov *et al.*, 2018; Baram *et al.*, 2017; Li *et al.*, 2017; Sharma *et al.*, 2018].

IL with the domain shifts

Using common measurable features is one of the popular approaches. For example, keypoints of objects [Sieb *et al.*, 2019] and/or tracking marker positions [Gupta *et al.*, 2016; Lee *et al.*, 2019b] are used as the states. In this approach, one can directly apply existing IL techniques without focusing on the domain shifts. However, such features are not always available. Stadie *et al.* added the domain confusion loss to the expert discriminator to make it domain-agnostic [Stadie *et al.*, 2017]. By computing the imitation reward using the discriminator, they successfully achieved IL with large domain shifts. Their approach, however, does not include SRL.

3 Proposed Method

3.1 Concept of proposed method

Figure 2 (a) shows a concept of DAC-SSM. \mathcal{D}_e represents the expert discriminator which serves as an imitation reward function. Because DAC-SSM builds domain-agnostic state space, higher rewards are provided to the agents for expert-like behavior. On the other hand, the existing method builds domain-aware state space. The expert discriminator easily distinguishes the states from the agents even when the behavior of the agents is expert-like.

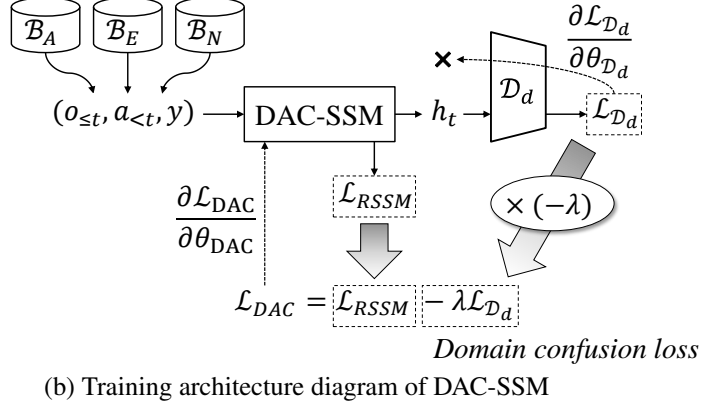
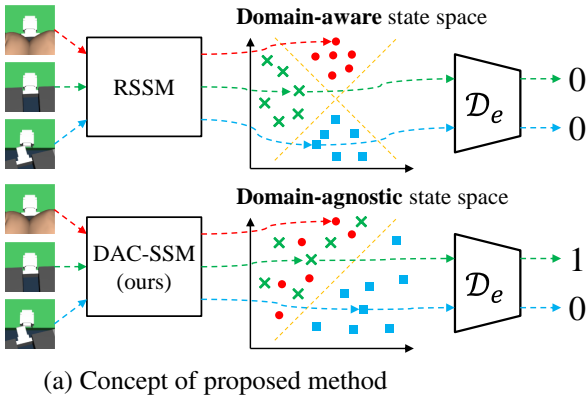


Figure 2: (a) Concept of proposed method. \mathcal{D}_e represents the expert discriminator which serves as an imitation reward function. Red, green and blue arrows represent the flows of states inference and computation of imitation rewards. The red arrow is for the expert data. The green arrow is for the agent data whose behavior is expert-like. The blue arrow is for the agent data whose behavior is NOT expert-like. (b) Training architecture of DAC-SSM. The dashed lines represent back-propagation paths. The domain confusion losses $-\lambda\mathcal{L}_{\mathcal{D}_d}$ are added to the state space losses \mathcal{L}_{RSSM} . \mathcal{B}_A , \mathcal{B}_E , and \mathcal{B}_N represent replay buffers for the data from the agents, experts, and novices. \mathcal{D}_d represents the domain discriminator.

3.2 State space model

In POMDPs, an individual image does not have all the information about the states. Therefore, our model builds on RSSM, which has contextual states to propagate historical information. We use the following notations: a discrete time step, t , contextual deterministic states, h_t , stochastic states, s_t , image observations, o_t , continuous actions, a_t , and domain labels, y . The model follows the mixed deterministic/stochastic dynamics below:

- Transition model: $h_t = f(h_{t-1}, s_{t-1}, a_{t-1})$
- State model: $s_t \sim p(s_t|h_t)$
- Observation model: $o_t \sim p(o_t|h_t, s_t, y)$

Transition model $f(h_{t-1}, s_{t-1}, a_{t-1})$ was implemented as a recurrent neural network. To train the model, we maximized the probability of a sequence of observations in the entire generative process:

$$p(o_{1:T}|a_{1:T}) = \int \prod_t [p(s_t|h_t)p(o_t|h_t, s_t, y)] ds_{1:T} \quad (1)$$

$$\text{where } h_t = f(h_{t-1}, s_{t-1}, a_{t-1})$$

Generally this objective is intractable. We utilize the following evidence lower bound (ELBO) on the log-likelihood by introducing the posterior $q(s_{t-1}|o_{\leq t-1}, a_{< t-1}, y)$ to infer the approximate stochastic states.

$$\begin{aligned} & \ln p(o_{1:T}|a_{1:T}) \\ & \geq \sum_{t=1}^T \mathbb{E}_{q(s_t|o_{\leq t}, a_{< t}, y)} [\ln p(o_t|h_t, s_t, y)] \\ & \quad - \mathbb{E}_{q(s_{t-1}|o_{\leq t-1}, a_{< t-1}, y)} [\text{KL}[q(s_t|o_{\leq t}, a_{< t}, y)||p(s_t|h_t)]] \\ & = -\mathcal{L}_{RSSM} \end{aligned} \quad (2)$$

The posterior $q(s_{t-1}|o_{\leq t-1}, a_{< t-1}, y)$ and the observation model $p(o_t|h_t, s_t, y)$ are implemented as an encoder and de-

coder, respectively. They are conditioned on the domain labels, y . The domain labels help them to change their behavior depending on the domain. The domain-dependent information is eliminated from the obtained states s_t and h_t , like CVAE.

3.3 Domain and expert discriminators

We further introduce the domain and expert discriminators, \mathcal{D}_d and \mathcal{D}_e . The role of the domain discriminator is for computing the domain confusion losses. We denote the replay buffers for the data from the agents, experts, and novices as \mathcal{B}_A , \mathcal{B}_E , and \mathcal{B}_N , respectively. The data from the novices are in the same domain as those from the experts, but are non-optimal for the tasks. The loss function of the domain discriminator is denoted as follows:

$$\begin{aligned} \mathcal{L}_{\mathcal{D}_d} = & \mathbb{E}_{h_t \sim \mathcal{B}_A} [\ln \mathcal{D}_d(h_t)] \\ & + \mathbb{E}_{h_t \sim \mathcal{B}_E} [\ln(1 - \mathcal{D}_d(h_t))] \\ & + \mathbb{E}_{h_t \sim \mathcal{B}_N} [\ln(1 - \mathcal{D}_d(h_t))] \end{aligned} \quad (3)$$

Here, we introduce a simple abbreviation of the expectation to avoid complexity:

$$\mathbb{E}_{h_t \sim \mathcal{B}} [\cdot] \equiv \mathbb{E}_{o_{\leq t-1}, a_{< t-1}, y \sim \mathcal{B}} \mathbb{E}_{s_{t-1} \sim q(s_{t-1}|o_{\leq t-1}, a_{< t-1}, y)} [\cdot]_{h_t = f(h_{t-1}, s_{t-1}, a_{t-1})} \quad (4)$$

Similarly, the loss function of the expert discriminator is denoted as follows:

$$\begin{aligned} \mathcal{L}_{\mathcal{D}_e} = & \mathbb{E}_{h_t, a_t \sim \mathcal{B}_A} [\ln \mathcal{D}_e(h_t, a_t)] \\ & + \mathbb{E}_{h_t, a_t \sim \mathcal{B}_E} [\ln(1 - \mathcal{D}_e(h_t, a_t))] \\ & + \mathbb{E}_{h_t, a_t \sim \mathcal{B}_N} [\ln \mathcal{D}_e(h_t, a_t)] \end{aligned} \quad (5)$$

The expert discriminator serves as an imitation reward function. It is trained to distinguish if state-action pairs (h_t, a_t) are from episodes of the experts or not.

3.4 Training of DAC-SSM

Figure 2 (b) displays a diagram of training architecture of DAC-SSM. The dashed lines represent back-propagation paths. The model is trained by minimizing state space losses with the domain confusion losses:

$$\mathcal{L}_{DAC} = \mathcal{L}_{RSSM} - \lambda \mathcal{L}_{\mathcal{D}_d} \quad (6)$$

where λ is a hyper-parameter. The reward models, r , are trained by the losses:

$$\mathcal{L}_r = - \sum_{t=1}^T \mathbb{E}_{q(s_t|o_{\leq t}, a_{< t}, y)} [\ln p(r_t|h_t, s_t)] \quad (7)$$

The gradient of the expert discriminator losses, $\partial \mathcal{L}_{\mathcal{D}_e} / \partial \theta_{\mathcal{D}_e}$, is not propagated to DAC-SSM. The gradient of the domain discriminator losses, $\partial \mathcal{L}_{\mathcal{D}_d} / \partial \theta_{\mathcal{D}_d}$, is not propagated to DAC-SSM directly, but the domain confusion losses, $-\lambda \mathcal{L}_{\mathcal{D}_d}$, are added to the state space losses, \mathcal{L}_{RSSM} . Thus, the obtained states become domain-agnostic, and task- and dynamics-aware. Therefore, the states have considerable information that is useful for control (task- and dynamics-aware), but few clues regarding the domain-dependent information (domain-agnostic). We prepared two types of datasets for each task: expert and novice data. Expert data are successful trajectories for tasks in the expert domain, whereas novice data are non-optimal trajectories for tasks in the expert domain. Agent data are collected during training.

3.5 Planning algorithm

We used the cross entropy method (CEM) [Chua *et al.*, 2018] to search for the best action sequence in the obtained state space. CEM is a robust population-based optimization algorithm that infers a distribution over action sequences that maximize an objective. Because the objective is modeled as a function of the states and actions, the planner can operate purely in the low-dimensional latent space without generating images. Multiple types of rewards are used for the objective [Kinose and Taniguchi, 2019; Kaushik *et al.*, 2018] in the context of control as inference [Levine, 2018]. We define the distribution over the task-optimality, \mathcal{O}_t^R , as follows:

$$p(\mathcal{O}_t^R = 1|h_t, s_t) = \exp(\mathbb{E}[p(r_t|h_t, s_t)]) \quad (8)$$

The distribution over the imitation-optimality, \mathcal{O}_t^I , is calculated by using the expert discriminator:

$$p(\mathcal{O}_t^I = 1|h_t, a_t) = \exp(\ln \mathcal{D}_e(h_t, a_t)) = \mathcal{D}_e(h_t, a_t) \quad (9)$$

We use h_t to calculate both rewards because contextual information is essential for the POMDPs. Hence, the objective of the CEM is to maximize the probability of the task- and imitation-optimality, as given below:

$$\begin{aligned} & \ln p(\mathcal{O}_{1:H}^R = 1, \mathcal{O}_{1:H}^I = 1|h_t, s_t, a_t) \\ &= \sum_{t=1}^H [\mathbb{E}[p(r_t|h_t, s_t)] + \ln \mathcal{D}_e(h_t, a_t)] \end{aligned} \quad (10)$$

where H is the planning horizon of the CEM.

4 Experiments

4.1 Environments and hyperparameters

We considered three tasks in the MuJoCo physics simulator: Cup-Catch, Finger-Spin, and Connector-Insertion. Figure 3 shows the expert and agent domains for each task. For Finger-Spin, we make two different agent domains. One agent domain of Finger-Spin has different colors of objects and floors compared to the expert domain. The other agent domain of Finger-Spin also has a different viewing angle. It is difficult to train control policies by using only task rewards because all tasks here are the sparse reward type. Cup-Catch and Finger-Spin are instances of the DeepMind Control Suite [Yuval *et al.*, 2018]. We also built a new task, Connector-Insertion. The agent attempted to insert a connector to a socket. Constant rewards were obtained when the connector was in the socket. The position and angle of the connector and socket were initialized with random values at the start of the episodes. In this task, we added a constant bias to the action of moving the connector upward on the paper. This is equivalent to introducing domain knowledge that the socket exists upward on the paper.

The contextual state and stochastic state sizes were 32 and 8 for all experiments. A small latent size is enough for DAC-SSM because domain-related information is eliminated from the latent space. The decoder refers to the domain labels to reconstruct domain-specific observation. Domain label y was simply concatenated to h_t and s_t and entered into the domain conditional (DC) decoder. We used not only the DC decoder but also the DC encoder for the Finger-Spin of the tilted view. We implemented the DC encoder by training two separate encoders and switching them based on domain label y . We use batches of 40 sequence chunks of 40 steps long for training. Except for the above mentioned, we adopted the same hyperparameters and architectures as PlaNet for the state space model. We implemented both the expert and domain discriminator as two fully connected layers of size 64 with ReLU activations. The domain confusion loss coefficient λ is 1.0 unless otherwise noted. For planning, we used CEM with a short planning horizon length of $H = 3$, optimization iterations of $I = 10$, candidate samples of $J = 4000$, and refitting to the best $K = 20$. The action repeats were 4, 2, and 800 for Cup-Catch, Finger-Spin, and Connector-Insertion, respectively. The action repeat for Connector-Insertion was extremely large because we set simulation timesteps of MuJoCo to a very small value of 5×10^{-5} ; otherwise, objects easily pass through each other when they come into forceful contact. We evaluate three types of objectives for the planning: dual, imitation and task rewards. The dual rewards are weighted sum of task- and imitation-rewards with ratio of 10:1.

4.2 Applying state representation to IL with domain shifts

Figure 4 and Table 1 compares DAC-SSM using dual rewards (DAC/dual) to a baseline of existing SRL method (PlaNet/task) and naive implementation of the expert discriminator with the baseline (PlaNet+ \mathcal{D}_e). DAC/dual achieved much higher performance for all tasks than the two baselines. This is because the domain-aware state repre-

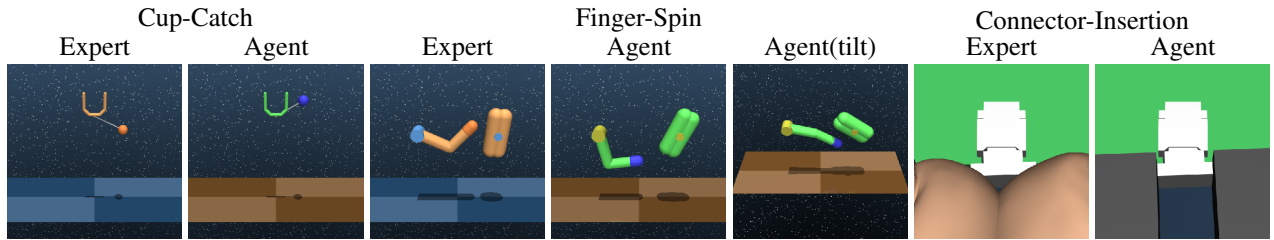


Figure 3: We consider three tasks: Cup-Catch, Finger-Spin, and Connector-Insertion. We consider two agent domains for Finger-Spin. In one agent domain, colors of bodies and floors are different from the expert domain. In the other agent domain, viewing angles are further different. In the Connector-Insertion, human fingers hold the connector in the expert domain, while robot fingers hold it in the agent domain.

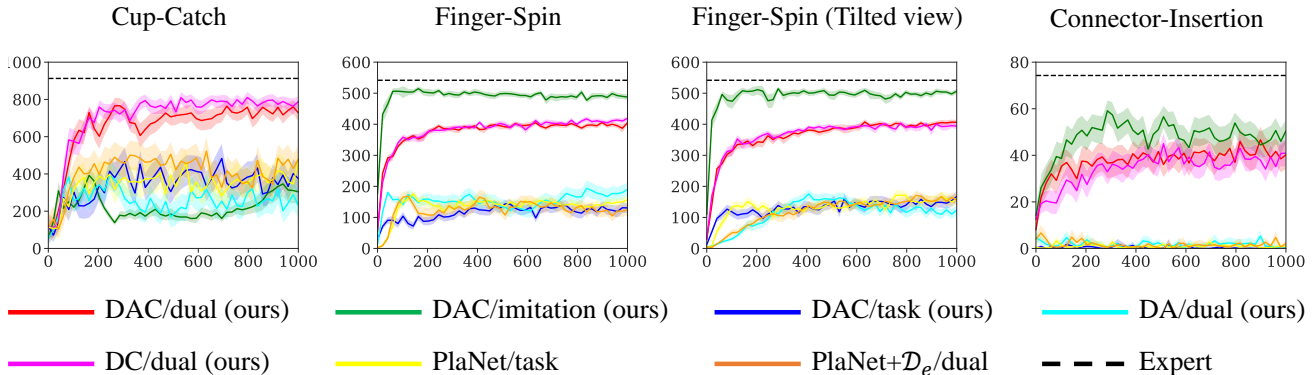


Figure 4: Comparison of our proposed method with the baselines. The plots show the test performance over the number of collected episodes. The lines show the medians, and the areas show the percentiles from 5 to 95 over 4 seeds and 20 trajectories. The dashed lines show the average scores of the expert trajectories. We compare DAC-SSM with three types of reward function: *task*, *imitation* and *dual*. The *dual* means weighted sum of the *task* and *imitation* rewards. DAC-SSM: with the domain confusion loss and the DC decoder. DA-SSM: with the domain confusion loss without the DC decoder. DC-SSM: without the domain confusion loss with the DC decoder. We used not only a DC decoder but also a DC encoder for the Finger-Spin of the tilted view. PlaNet+ \mathcal{D}_e : naive implementation of the expert discriminator and RSSM.

sensation of PlaNet does not help the agents to achieve higher performance via imitation learning with the domain shifts. We also compared DAC-SSM, a version using dual rewards (DAC/dual), a version using imitation rewards (DAC/imitation), and a version using task rewards (DAC/task). Except for Cup-Catch, DAC/imitation achieved the best performance. This is because the planning horizon length $H = 3$ is too short for Finger-Spin and Connector-Insertion. We further trained our proposed model (DAC/dual) as well as versions with domain adversarial training but *without* domain conditional encoders/decoders (DA/dual), and with domain conditional encoders/decoders but *without* domain adversarial training (DC/dual). The performance of DAC/dual and DC/dual were almost the same, and that of DA/dual was much lower. In the settings of this experiment, the domain adversarial training was not effective because the domain confusion loss coefficient $\lambda = 1$ was too small. Table 2 shows DAC/dual achieved higher performance than DC/dual with $\lambda = 3$ for Connector-Insertion. These results show that the obtained states on DAC-SSM help the agents to achieve effective imitation learning with the domain shifts.

4.3 Reconstruction from State Representation

Figure 5 shows the sequence of ground-truth examples and reconstructed images from the obtained state representation on DAC-SSM for Finger-Spin. The first 5 columns show context frames that were reconstructed from posterior samples, and the remaining images were generated from open-loop prior samples. The second and third row images were reconstructed from a sequence of states of h_t and s_t with domain label y via the DC-decoder $p(o_t|h_t, s_t, y)$. Joint angles of the robotic arm and target object were successfully reconstructed from the states, whereas domain-dependent information (colors of the floor and object) depended on the domain labels. The last row images were reconstructed from the contextual states, h_t , *without* domain labels using another decoder that is trained separately from our model. The joint angles were successfully reconstructed, whereas the colors appeared to be a mixture of the two domains. These results show that the obtained states on DAC-SSM have control-dependent information like the joint-angle, but do not have domain-dependent information like the colors which is not related to the control. In other words, we successfully acquire the domain-agnostic and task- and dynamics-aware state representation via DAC-SSM.

Task	DAC/dual	DAC/imitation	DAC/task	DA/dual	DC/dual	PlaNet	PlaNet+ \mathcal{D}_e
Cup-Catch	728±223	304±323	375±371	233±350	788±149	470±398	479±359
Finger-Spin	405±42	488±50	130±73	190±108	419±41	157±73	124±91
Finger-Spin (tilted view)	406±45	507±48	167±87	123±80	394±51	162±87	156±89
Connector- Insertion	40.2±29.1	50.5±25.0	0.4±4.0	0.0±0.0	40.9±26.7	0.7±3.4	2.1±8.1

Table 1: Mean MPC performance after 1,000 episodes, boldface indicates better results, \pm represents one standard deviation.

Task	DC/dual $\lambda = 0$	DAC/dual $\lambda = 0.1$	DAC/dual $\lambda = 0.3$	DAC/dual $\lambda = 1.0$	DAC/dual $\lambda = 3.0$	DAC/dual $\lambda = 10.0$
Finger-Spin	419±41	417±45	409±47	405±42	337±52	1±2
Connector-Insertion	40.9±26.7	35.3±28.4	37.4±29.6	40.2±29.1	49.5±25.5	17.3±23.8

Table 2: Mean MPC performance for different domain confusion loss coefficient λ after 1,000 episodes, boldface indicates better results, \pm represents one standard deviation.

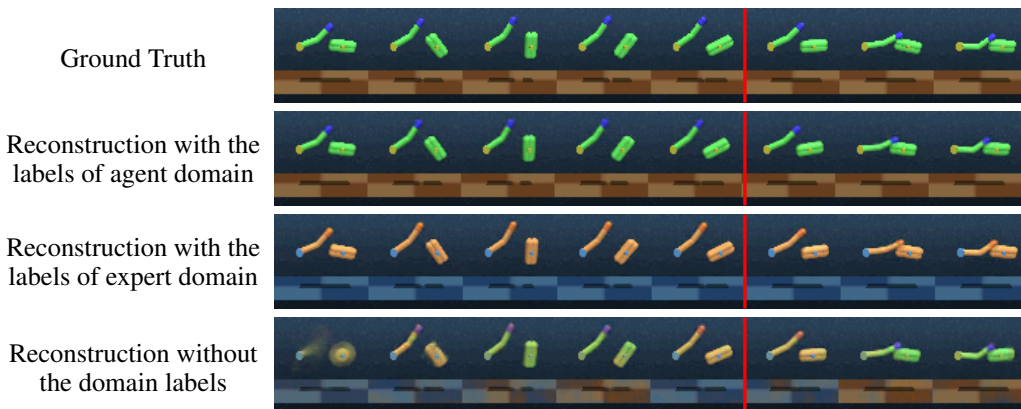


Figure 5: Example image sequence (the first row) and corresponding open-loop video predictions (second to the last row) observed for the Finger-Spin task. Columns 1-5 are context frames and were reconstructed from posterior samples, and the remaining images were generated from open-loop prior samples. The second and third row was reconstructed with expert and agent domain labels, respectively. The last row was reconstructed from the contextual states, h_t , *without* domain labels. Another decoder was trained separately for the reconstruction of the images in the last row. The first column of the last row is reconstructed from h_t initialized by zero.

5 Conclusion and Discussions

We showed domain-agnostic and task- and dynamics-aware state representation was obtained via DAC-SSM. To obtain such state representation, we introduced domain adversarial training and domain conditional encoders/decoders into the recent task- and dynamics-aware sequential state space model. Moreover, we experimentally evaluated the MPC performance via IL with the large domain shifts for continuous control sparse reward tasks in simulators. The state representation from DAC-SSM helped the agents to achieve comparable performance to the expert. The existing SRL failed to remove domain-dependent information from the states, and thus the agents could not perform effective IL with large domain shifts. We conclude that the domain-agnostic and control-aware states are essential for IL with the large domain shifts, and such states are obtained via DAC-SSM.

A question that remains is if DAC-SSM is applicable to larger and/or different types of domain shifts, e.g. modality-variant of data. Since the domain confusion loss coefficient

λ has task dependency as shown in Table 2, we can expect better state representation is obtained by actively varying λ . Acquiring task-agnostic states to achieve a universal controller is also appealing future works. Learning from human demonstration is challenging but interesting direction of future works. This work includes obtaining appropriate state representation from expert data *without* action data. Implementation for real robotic tasks is another important direction for future works. Acquiring fully stochastic state representation is necessary for the real world tasks because the control system of the real robot have much larger uncertainty than simulation.

Acknowledgments

Most of the experiments were conducted in ABCI (AI Bridging Cloud Infrastructure), built by the National Institute of Advanced Industrial Science and Technology, Japan.

References

- [Baram *et al.*, 2017] Nir Baram, Oron Ansel, Itai Caspi, and Shie Mannor. End-to-end differentiable adversarial imitation learning. In *ICML*, 2017.
- [Chua *et al.*, 2018] Kurtland Chua, Roberto Calandra, Rowan McAllister, and Sergey Levine. Deep reinforcement learning in a handful of trials using probabilistic dynamics models. In *NIPS*, 2018.
- [Gangwani *et al.*, 2019] Tanmay Gangwani, Joel Lehman, Qiang Liu, and Jian Peng. Learning belief representations for imitation learning in pomdps. In *UAI*, 2019.
- [Ganin *et al.*, 2015] Yaroslav Ganin, Evgeniya Ustinova, Hana Ajakan, Pascal Germain, Hugo Larochelle, François Laviolette, Mario Marchand, and Victor S. Lempitsky. Domain-adversarial training of neural networks. In *J. Mach. Learn. Res.*, volume 17, pages 59:1–59:35, 2015.
- [Garcia *et al.*, 1989] C. E. Garcia, D. M. Prett, and M. Morari. Model predictive control: Theory and practice—a survey. In *Automatica*, 1989.
- [Gonzalez-Garcia *et al.*, 2018] Abel Gonzalez-Garcia, Joost van de Weijer, and Yoshua Bengio. Image-to-image translation for cross-domain disentanglement. In *NIPS*, 2018.
- [Goodfellow *et al.*, 2014] Ian J. Goodfellow, Jean Pouget-Abadie, Mehdi Mirza, Bing Xu, David Warde-Farley, Sherjil Ozair, Aaron Courville, and Yoshua Bengio. Generative adversarial nets. In *NIPS*, 2014.
- [Gupta *et al.*, 2016] Abhishek Gupta, Clemens Eppner, Sergey Levine, and Pieter Abbeel. Learning dexterous manipulation for a soft robotic hand from human demonstrations. In *IROS*, 2016.
- [Ha and Schmidhuber, 2018] David Ha and Jürgen Schmidhuber. Recurrent world models facilitate policy evolution. In *NIPS*, 2018.
- [Hafner *et al.*, 2018] Danijar Hafner, Timothy Lillicrap, Ian Fischer, Ruben Villegas, David Ha, Honglak Lee, and James Davidson. Learning latent dynamics for planning from pixels. In *arXiv*, 2018.
- [Ho and Ermon, 2016] Jonathan Ho and Stefano Ermon. Generative adversarial imitation learning. In *NIPS*, 2016.
- [Kaushik *et al.*, 2018] Rituraj Kaushik, Konstantinos Chatzilygeroudis, and Jean-Baptiste Mouret. Multi-objective model-based policy search for data-efficient learning with sparse rewards. In *CoRL*, 2018.
- [Kingma *et al.*, 2014] Diederik Kingma, Danilo Rezende, Shakir Mohamed, and Max Welling. Semi-supervised learning with deep generative models. In *NIPS*, 2014.
- [Kinose and Taniguchi, 2019] Akira Kinose and Tadahiro Taniguchi. Integration of imitation learning using gail and reinforcement learning using task-achievement rewards via probabilistic generative model. In *arXiv*, 2019.
- [Kostrikov *et al.*, 2018] Ilya Kostrikov, Kumar Krishna Agrawal, Debidatta Dwibedi, Sergey Levine, and Jonathan Tompson. Discriminator-actor-critic: Addressing sample inefficiency and reward bias in adversarial imitation learning. In *ICLR*, 2018.
- [Lee *et al.*, 2019a] Alex X. Lee, Anusha Nagabandi, Pieter Abbeel, and Sergey Levine. Stochastic latent actor-critic: Deep reinforcement learning with a latent variable model. In *arXiv*, 2019.
- [Lee *et al.*, 2019b] Youngwoon Lee, Edward S. Hu, Zhengyu Yang, and Joseph J. Lim. To follow or not to follow: Selective imitation learning from observations. In *CoRL*, 2019.
- [Lesort *et al.*, 2018] Timothée Lesort, Natalia Díaz-Rodríguez, Jean-François Goudou, and David Filliat. State representation learning for control: An overview. In *Neural Networks*, volume 108, 2018.
- [Levine, 2018] Sergey Levine. Reinforcement learning and control as probabilistic inference: Tutorial and review. In *arXiv*, 2018.
- [Li *et al.*, 2017] Yunzhu Li, Jiaming Song, and Stefano Ermon. Infogail: Interpretable imitation learning from visual demonstrations. In *NIPS*, 2017.
- [Okada and Taniguchi, 2019] Masashi Okada and Tadahiro Taniguchi. Variational inference mpc for bayesian model-based reinforcement learning. In *CoRL*, 2019.
- [Schaal, 1999] Stefan Schaal. Is imitation learning the route to humanoid robots? In *Trends in Cognitive Sciences*, volume 3, 1999.
- [Sharma *et al.*, 2018] Arjun Sharma, Mohit Sharma, Nicholas Rhinehart, and Kris M. Kitani. Directed-info gail: Learning hierarchical policies from unsegmented demonstrations using directed information. In *arXiv*, 2018.
- [Sieb *et al.*, 2019] Maximilian Sieb, Zhou Xian, Audrey Huang, Oliver Kroemer, and Katerina Fragkiadaki. Graph-structured visual imitation. In *CoRL*, 2019.
- [Stadie *et al.*, 2017] Bradley C. Stadie, Pieter Abbeel, and Ilya Sutskever. Third-person imitation learning. In *ICLR*, 2017.
- [Todorov *et al.*, 2012] Emanuel Todorov, Tom Erez, and Yuval Tassa. Mujoco: A physics engine for model-based control. In *IROS*, 2012.
- [Torabi *et al.*, 2019] Faraz Torabi, Garrett Warnell, and Peter Stone. Recent advances in imitation learning from observation. In *IJCAI*, 2019.
- [Tzeng *et al.*, 2014] Eric Tzeng, Judy Hoffman, Ning Zhang, Kate Saenko, and Trevor Darrell. Deep domain confusion: Maximizing for domain invariance. In *arXiv*, 2014.
- [Wang *et al.*, 2019] Angelina Wang, Thanard Kurutach, Kara Liu, Pieter Abbeel, and Aviv Tamar. Learning robotic manipulation through visual planning and acting. In *RSS*, 2019.
- [Yuval *et al.*, 2018] Tassa Yuval, Doron Yotam, Muldal Al-istair, Erez Tom, Li Yazhe, de Las Casas Diego, Budden David, Abdolmaleki Abbas, Merel Josh, Lefrancq Andrew, Lillicrap Timothy, and Riedmiller Martin. Deepmind control suite. In *arXiv*, 2018.